

Locally finite amplitude for multi Higgs production in gluon fusion at two loops

Julia Karlen^{a,*}

^a*Institute for Theoretical Physics, ETH Zurich,
8093 Zürich, Switzerland*

E-mail: karlenj@phys.ethz.ch

A universal numerical approach for computing loop amplitudes would permit to achieve high precision in theoretical predictions for a wide range of phenomenologically relevant processes. A major obstacle in developing such methods is the treatment of local infrared and ultraviolet singularities. These need to be removed at the integrand level before numerical integration becomes feasible. In these proceedings we discuss a framework under development for the construction of locally finite two-loop amplitudes for arbitrary processes. It is based on the universality of infrared singularities, realizing infrared factorization manifestly in momentum space. As a specific example, the construction of the locally finite two-loop amplitude for single Higgs production in gluon fusion is discussed in detail. It generalizes to the production of an arbitrary number of electroweak final states in gluon fusion [15].

Loops and Legs in Quantum Field Theory (LL2024)
14-19, April, 2024
Wittenberg, Germany

*Speaker

1. Introduction

Over the past few decades, immense efforts have been made to calculate two-loop amplitudes for relevant processes at the LHC [1]. To further increase the precision of collider phenomenology, the introduction of additional kinematic or mass scales in two-loop scattering amplitudes is necessary [2]. This prompts the development of methods that are less sensitive to the number of masses in internal or external particles. One attractive approach is computing multi-loop amplitudes numerically directly in momentum space, as this technique keeps the number of integrations per loop order constant, regardless of the number of external legs or kinematic scales. However the numerical integration of an amplitude in momentum space is not straightforward. Ultraviolet and infrared singularities need to be removed at the local level of the integrand before the amplitude is amenable to numerical integration.¹ In these proceedings we present a framework that exploits the factorization properties of scattering amplitudes to construct hard functions for two-loop amplitudes locally in momentum space.

Notably, wide-angle scattering amplitudes in gauge theories factorize to all orders in perturbation theory into a soft function, jet functions and a hard function [4–12].

$$M = \text{Soft} \cdot \prod_i \text{Jet}_i \cdot \text{Hard}, \quad (1)$$

where all the soft divergences of M are in the soft function, all the collinear divergences are in the jet functions, and the hard function is infrared finite. Note that the soft and jet functions are universal functions, while the remaining process dependence is stored in the hard function, which describes interactions at short distances. With this construction, one can imagine assembling the infrared singular parts of an amplitude with any number of colorless final states from simpler, already known processes, such as form factors. The remainder, which is locally finite, can then be integrated numerically. Namely,

$$M = \int d[k] \mathcal{M} = \int d[k] \underbrace{\mathcal{S} \cdot \prod_i \mathcal{J}_i}_{\equiv \mathcal{F}, \text{ form factor}} \int d[k] \underbrace{\mathcal{M} \cdot \mathcal{S}^{-1} \cdot \prod_i \mathcal{J}_i^{-1}}_{\equiv \mathcal{H}, \text{ IR-finite}} \quad (2)$$

where the script letters denote the integrands and $\int d[k]$ denotes the integration over all loop momenta. For hadron collider processes with colorless final states the soft function is not a matrix and we can combine it with the jet function into a form factor \mathcal{F} . Order by order in perturbation theory the hard function at the integrand level therefore is

$$\begin{aligned} \mathcal{H}^{(0)} &= \mathcal{M}^{(0)}, \\ \mathcal{H}^{(1)} &= \mathcal{M}^{(1)} - \mathcal{F}^{(1)} \mathcal{M}^{(0)}, \\ \mathcal{H}^{(2)} &= \mathcal{M}^{(2)} - \mathcal{F}^{(1)} \mathcal{H}^{(1)} - \mathcal{F}^{(2)} \mathcal{M}^{(0)}. \end{aligned} \quad (3)$$

To construct a fully finite hard function at the local level further modifications are necessary. The reason for this is that factorization properties are symmetric expressions (e.g. under gauge

¹Note that additional treatment of threshold singularities are further required to successfully integrate directly in momentum space. For ongoing efforts on this topic, see for example Matilde Vicini's talk [3].

symmetries of the theory) and such symmetries are not always manifest at the integrand level. The full infrared factorization in momentum space has so far been developed for two collections of processes at two loops, namely off-shell photon production in electron positron annihilation [13] and electroweak production in quark anti-quark annihilation [14].

In these proceedings we will focus on the two-loop amplitudes for gluon fusion to colorless, electroweak final states, via a heavy quark loop which is based on ref. [15]. In particular we will discuss the two-loop amplitude of single Higgs production for a more pedagogical introduction to this topic. This is a next-to-leading order process. The leading order is a heavy quark loop one-loop amplitude and does not entail any infrared singularities. The two-loop hard function amenable to numerical integration takes the following form:

$$\mathcal{H}_{gg \rightarrow H}^{(2),R}(k, l) = \mathcal{M}_{gg \rightarrow H}^{(2),R}(k, l) - \mathcal{F}_{\text{scalar}}^{(1),R}(k) \mathcal{M}_{gg \rightarrow H}^{(1),R}(l) - \Delta \mathcal{M}_{gg \rightarrow H}^{(2),R}(k, l), \quad (4)$$

where the superscript R indicates the subtraction of local ultraviolet counterterms. The superscript $m = 1, 2$ indicates the loop order of the amplitude or the counterterms, and the subscript $gg \rightarrow H$ indicates the process. All of the infrared singularities are contained in a one-loop “scalar” form factor independent of the incoming gluon spin states. The terminology of “scalar” is discussed in section 2.1. The momenta k and l are the loop momenta. It is important to mention that eq. (4) is valid for an arbitrary number of electroweak final states [15]. Note that an additional counterterm $\Delta \mathcal{M}_{gg \rightarrow H}^{(2),R}(k, l)$ compared to eq. (3) is necessary to make the infrared factorization manifestly local in loop momentum space. This counterterm does not change the value of the integrated amplitude since it integrates to zero

$$\int dl^D \Delta \mathcal{M}_{gg \rightarrow H}^{(2),R}(k, l) = 0. \quad (5)$$

It does, however, ensure the cancellation of loop momentum mismatches in one-loop hard subdiagrams that occur in collinear limits, thus allowing Ward identities to be implemented locally. In section 2 we introduce a decomposition of the triple-gluon vertex named “scalar” decomposition. The decomposition allows for a natural classification of the infrared singular diagrams of the amplitude into two distinct classes, with respect to their behavior in the infrared limits. Additionally it allows to introduce appropriate gluon momentum labels necessary for the factorization to emerge locally. In section 3, the factorization of the first class of diagrams locally in momentum space is demonstrated via the use of Ward identities. The remaining class of diagrams, which do not directly contribute to factorization, is discussed in section 4. These diagrams are finite after integration, but have local infrared singularities. For numerical integration, we will introduce additional counterterms of the form outlined in eq. (5). Finally, we conclude the paper and discuss some further steps towards a general framework in section 5.

2. General setup

To achieve the local factorization in eq. (4), the infrared behavior of the amplitude needs to be studied. Below the infrared singular Feynman diagrams contributing to the two-loop amplitude for

single Higgs production in gluon fusion are listed

$$\mathcal{M}_{\text{IR}, gg \rightarrow H}^{(2)} =$$

Each of these singular diagrams has a triple-gluon vertex, which is the origin of infrared singularities (collinear and soft). Each term in the triple-gluon vertex exhibits a different behavior in the collinear limits. Moreover, they play different roles in the cancellations between diagrams in the collinear limits, which eventually lead to the factorization of the collinear singularities. To systematically study infrared singularities in collinear and soft limits, it is useful to decompose the triple gluon vertex.

2.1 “Scalar” decomposition

Noticing that each term in the triple-gluon vertex corresponds to the tree-level Feynman rule for the interaction of color-octet “scalars” and a gluon times the metric, $\eta^{\alpha\beta}$, we graphically decompose the triple gluon vertex as

$$\begin{aligned} & \begin{array}{c} \gamma, c \\ \downarrow k_3 \\ \alpha, a \text{-----} \beta, b \\ \leftarrow k_1 \quad \rightarrow k_2 \end{array} = -g_s f_{abc} (k_1 - k_2)^\gamma \eta^{\alpha\beta} - g_s f_{bca} (k_2 - k_3)^\alpha \eta^{\beta\gamma} - g_s f_{cab} (k_3 - k_1)^\beta \eta^{\gamma\alpha} \\ & = \begin{array}{c} \gamma, c \\ \downarrow k_3 \\ \alpha, a \text{-----} \beta, b \\ \leftarrow k_1 \quad \rightarrow k_2 \end{array} + \begin{array}{c} \gamma, c \\ \downarrow k_3 \\ \alpha, a \text{-----} \beta, b \\ \leftarrow k_1 \quad \rightarrow k_2 \end{array} + \begin{array}{c} \gamma, c \\ \downarrow k_3 \\ \alpha, a \text{-----} \beta, b \\ \leftarrow k_1 \quad \rightarrow k_2 \end{array}, \end{aligned} \quad (6)$$

where each term on the right-hand side of the first line corresponds, in order, to each term on the second line. This decomposition is denoted as a “scalar” decomposition. As an example, the “scalar” decomposition of one infrared singular diagram is given

$$\begin{array}{c} p_1 \text{-----} \\ \swarrow \quad \searrow \\ \text{---} \quad \text{---} \\ \swarrow \quad \searrow \\ p_2 \text{-----} \end{array} = \begin{array}{c} p_1 \text{-----} \\ \swarrow \quad \searrow \\ \text{---} \quad \text{---} \\ \swarrow \quad \searrow \\ p_2 \text{-----} \end{array} + \begin{array}{c} p_1 \text{-----} \\ \swarrow \quad \searrow \\ \text{---} \quad \text{---} \\ \swarrow \quad \searrow \\ p_2 \text{-----} \end{array} + \begin{array}{c} p_1 \text{-----} \\ \swarrow \quad \searrow \\ \text{---} \quad \text{---} \\ \swarrow \quad \searrow \\ p_2 \text{-----} \end{array}. \quad (7)$$

It is important to note that the dashed lines still describe gluons and only graphically indicate which triple-gluon vertex term is being considered. Therefore, a dashed propagator is a gluon propagator, a “scalar”-quark vertex should be read with the same Feynman rules as a gluon-quark vertex and an external “scalar” remains an external gluon. The last diagram in this decomposition is infrared finite, due to the transversality of the polarization vector. Applying the Feynman rules, we find that

the diagram is proportional to $\epsilon(p_1) \cdot (2k + p_1)$, which is zero in the limit where $k \parallel p_1$. We will omit this diagram from the collection of IR singular diagrams from now on.

Analyzing the infrared singularities of the amplitude in detail, we find that for infrared factorization to be manifest at the integrand level, the gluons must always have the same momentum label. The original momentum flow of the diagram displayed in eq. (7) therefore does not lead to local factorization. The ‘‘scalar’’ decomposition is particularly useful as it allows for the imposition of a different momentum flow for each decomposed diagram.

2.2 Classification

The ‘‘scalar’’ decomposition not only allows to implement the required gluon momentum labels, but also to classify the diagrams with respect to their behavior in the collinear limits. As already mentioned above, diagrams in which the incoming gluon splits into two ‘‘scalar’’ lines are infrared finite due to the transversality of the polarization vectors. The remaining infrared diagrams separate into two distinct groups. For each diagram in the first group, the collinear singularities factorize locally in the sum. Therefore, we call them *factorizable diagrams* and denote them as $\mathcal{M}_{\text{IR}, gg \rightarrow H}^{(2), \text{fact}}$:

$$\begin{aligned}
 \mathcal{M}_{\text{IR}, gg \rightarrow H}^{(2), \text{fact}} = & \text{Diagram 1} + \text{Diagram 2} + \text{Diagram 3} \\
 & + \text{Diagram 4} + \text{Diagram 5} + \text{Diagram 6} \\
 & + \text{Diagram 7} + \text{other charge flow} .
 \end{aligned} \tag{8}$$

The second set of diagrams we call *shift-integrable diagrams*, denoted by $\mathcal{M}_{\text{IR}, gg \rightarrow H}^{(2), \text{shift}}$:

$$\begin{aligned}
 \mathcal{M}_{\text{IR}, gg \rightarrow H}^{(2), \text{shift}} = & \text{Diagram 1} + \text{Diagram 2} + \text{Diagram 3} \\
 & + \text{Diagram 4} + \text{Diagram 5} + \text{Diagram 6} \\
 & + \text{Diagram 7} + \text{other charge flow} .
 \end{aligned} \tag{9}$$

In both classes, only one charge flow of the heavy quark loop is shown, and all gluons are labeled k flowing away from p_2 and/or into p_1 . Note that a ‘‘scalar’’-gluon propagator present in the diagrams above has the same Feynman rule as a gluon propagator, but the split allows to indicate which term

3.2 Local factorization

We will now study the factorization of the factorizable diagrams at the integrand level through Ward identity cancellations in the collinear limit $k \parallel p_1$. The local factorization requires not only a careful assignment of the gluon loop momentum through the ‘‘scalar’’ decomposition as discussed above, but also needs a careful assignment of the loop momentum in the heavy quark loop. As an example, we consider the third and fourth diagram in eq. (8) in the collinear limit $k \parallel p_1$:

$$\begin{aligned}
 & \text{Diagram 1} + \text{Diagram 2} \\
 = & \text{Diagram 3} + \text{Diagram 4} + \text{Diagram 5} + \text{Diagram 6} \quad (=0)
 \end{aligned} \tag{13}$$

The colored quark propagators on the first line indicate that these propagators require the same momentum labeling in both diagrams. Using the Ward identity in eq. (11), we note that the second and third diagrams on the second line are identical, except for the different sign of the vertex where the gluon attaches next to the Higgs boson via a double line defined in eq. (12). Thus, the two expressions cancel each other. Similarly, intermediate terms between the remaining diagrams in $\mathcal{M}_{\text{IR}, gg \rightarrow H}^{(2), \text{fact}}$ cancel in the collinear limit via the Ward identity in eq. (11) or the Ward identity arising from a longitudinally polarized gluon hitting a ‘‘scalar’’ line. This results in two external leg corrections to the diagram, thereby achieving factorization at the integrand level in this limit. Diagrammatically, this is represented as follows:

$$\lim_{k \parallel p_1} \mathcal{M}_{\text{IR}, gg \rightarrow H}^{(2), \text{fact}} = \text{Diagram 1} + \text{Diagram 2} + \text{other charge flow} . \tag{14}$$

A careful study of the color factors allows to write the factorizable diagrams in the limit as

$$\lim_{k \parallel p_1} \mathcal{M}_{\text{IR}, gg \rightarrow H}^{(2), \text{fact}} = -i g_s^2 \frac{C_A}{2} \frac{1}{k^2 (k + p_1)^2} \frac{(k + 2p_1) \cdot p_2}{k \cdot p_2} \left(\mathcal{M}_{gg \rightarrow H}^{(1)}(l) + \mathcal{M}_{gg \rightarrow H}^{(1)}(l + k) \right), \tag{15}$$

with the full one-loop amplitude $\mathcal{M}_{gg \rightarrow H}^{(1)}$, i.e. the heavy quark loop, with both charge flows. The finite one-loop amplitudes are averaged over two loop momentum flows, which are shifted by $l \rightarrow l + k$ with respect to each other. In the other collinear limit $k \parallel p_2$ the factorization occurs analogously. Lastly, the singular behavior in the soft limit, where $k \sim 0$, originates entirely from the first diagram in eq. (8) (and its other charge flow) and is equal to the soft limit of eq. (15).

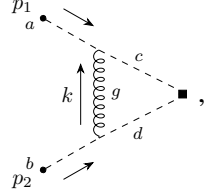
3.3 Form factor and shift counterterms

Motivated by the fact that the factorized collinear singularity of eq. (15) is also present in a gauge theory of scalars, we use an amplitude for a simple $2 \rightarrow 1$ scalar fusion process as an infrared

counterterm. It contains the same soft and collinear singularities as the diagrams in eq. (8), such that the local hard function can be written as

$$\mathcal{H}_{gg \rightarrow H, \text{IR}}^{(2), \text{fact}}(k, l) = \mathcal{M}_{gg \rightarrow H, \text{IR}}^{(2), \text{fact}}(k, l) - \mathcal{F}_{\text{scalar}}^{(1)}(k) \times \frac{1}{2} \left(\mathcal{M}_{gg \rightarrow H}^{(1)}(l) + \mathcal{M}_{gg \rightarrow H}^{(1)}(l+k) \right). \quad (16)$$

The scalar form factor is defined by

$$\mathcal{F}_{\text{scalar}}^{(1)}(k) \delta_{ab} = -i g_s^2 C_A \frac{(k-2p_2) \cdot (k+2p_1)}{k^2 (k+p_1)^2 (k-p_2)^2} \delta_{ab} = \text{diagram}, \quad (17)$$


where the color indices are included and the dots on the external legs imply that the polarization vectors are omitted. In the collinear limit $k \parallel p_1$ the second term on the right hand side of eq. (16) exactly matches the expression in eq. (15), such that when it is subtracted from the factorizable diagrams, the collinear singularity is removed.

Eq. (16) takes the form of eq. (4) if the additional counterterm $\Delta \mathcal{M}_{gg \rightarrow H}^{(2)}(k, l)$ in eq. (4) is

$$\Delta \mathcal{M}_{gg \rightarrow H, \text{IR}}^{(2), \text{fact}}(k, l) = \mathcal{F}_{\text{scalar}}^{(1)}(k) \times \frac{1}{2} \left(\mathcal{M}_{gg \rightarrow H}^{(1)}(l+k) - \mathcal{M}_{gg \rightarrow H}^{(1)}(l) \right), \quad (18)$$

where the superscript “fact” indicates that it is a counterterm for the factorizable diagrams. This is a difference of the form factor times the one-loop amplitude at two different values of its loop momentum. This difference integrates to zero and is called a *shift counterterm*. This concludes the discussion of the factorizable diagrams for which we demonstrated the local factorization as stated in eq. (4).

4. Shift-integrable diagrams

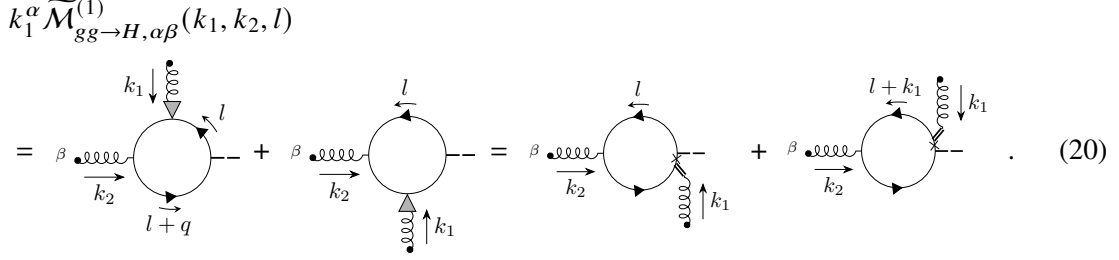
The shift-integrable diagrams given in eq. (9) are the remaining infrared singular diagrams resulting from the “scalar” decomposition. These diagrams are infrared finite after integration, because their infrared singularities cancel due to the QED Ward identity. However, to achieve local finiteness, we still need to subtract additional counterterms that vanish after integration, which we shall discuss in this section.

As a first step all soft singular terms can be removed by a counterterm that integrates to zero

$$\Delta_s \mathcal{M}_{gg \rightarrow H, \text{IR}}^{(2), \text{shift}} = i g_s^2 C_A \left(k_1^\alpha u_1^\beta + u_2^\alpha k_2^\beta + k_1^\alpha k_2^\beta \epsilon_1 \cdot \epsilon_2 \right) \frac{\widetilde{\mathcal{M}}_{gg \rightarrow H, \alpha\beta}^{(1)}(k_1, k_2, l)}{k^2 k_1^2 k_2^2}. \quad (19)$$

We define $k_1 \equiv k + p_1$ and $k_2 \equiv p_2 - k$ for legibility and denote the one-loop amplitude with two incoming gluons of momenta k_1 and k_2 and removed polarization vectors as $\widetilde{\mathcal{M}}_{gg \rightarrow H, \alpha\beta}^{(1)}(k_1, k_2, l)$. The vectors u_1^α and u_2^β depend on the loop momentum k , the external momenta p_1, p_2 and the polarization vectors ϵ_1, ϵ_2 and are not further relevant for the discussion. Note that for each term in the brackets, the counterterm is proportional to a longitudinally polarized gluon (with momentum k_1

or k_2) entering the heavy quark loop, i.e. the one-loop amplitude, everywhere. Since all diagrams have the same color factor, the QED Ward identity holds. For example,

$$k_1^\alpha \widetilde{\mathcal{M}}_{gg \rightarrow H, \alpha\beta}^{(1)}(k_1, k_2, l)$$


$$= \beta \text{ (diagram 1)} + \beta \text{ (diagram 2)} = \beta \text{ (diagram 3)} + \beta \text{ (diagram 4)} . \quad (20)$$

Applying the rules in eq. (12), we conclude that this is a difference of the same diagram with two different values of the loop momentum. Therefore, it vanishes after integration over the loop momentum l . Analogously, this also holds when the other gluon is longitudinally polarized

$$\int d^D l k_1^\alpha \widetilde{\mathcal{M}}_{gg \rightarrow H, \alpha\beta}^{(1)}(k_1, k_2, l) = \int d^D l k_2^\alpha \widetilde{\mathcal{M}}_{gg \rightarrow H, \alpha\beta}^{(1)}(k_1, k_2, l) = 0, \quad (21)$$

such that the counterterm $\Delta_s \mathcal{M}_{gg \rightarrow H, \text{IR}}^{(2), \text{shift}}$ can be removed from the amplitude without changing its integrated value. We can now examine the remaining collinear limits of the modified shift-integrable diagrams. In the collinear limit $k \parallel p_1$ we obtain

$$\lim_{k=-x p_1} \left(\mathcal{M}_{gg \rightarrow H, \text{IR}}^{(2), \text{shift}} - \Delta_s \mathcal{M}_{gg \rightarrow H, \text{IR}}^{(2), \text{shift}} \right) = 4 i g_s C_A \frac{x}{x-1} \frac{k_1^\alpha v_1^\beta \widetilde{\mathcal{M}}_{gg \rightarrow H, \alpha\beta}^{(1)}(k_1, k_2, l)}{k^2 k_1^2 k_2^2}, \quad (22)$$

where v_1^β depends on the loop momentum k , the external momentum p_2 and the polarization vectors and is not further relevant for the discussion. The modified shift-integrable diagrams become proportional to a longitudinally polarized gluon k_1 entering the heavy quark loop everywhere. Again the QED Ward identity in eq. (20) applies, resulting in a difference of the same diagram with two different values of the loop momentum. Hence, this is a non-local cancellation in the collinear limit and only vanishes after the integration over l . One has to remove this difference to be able to integrate the hard function numerically. This can be done by subtracting a counterterm of the form

$$\Delta_1 \mathcal{M}_{gg \rightarrow H, \text{IR}}^{(2), \text{shift}} = i g_s C_A \frac{k_1^\alpha v_1^\beta \widetilde{\mathcal{M}}_{gg \rightarrow H, \alpha\beta}^{(1)}(k_1, k_2, l)}{k^2 k_1^2} \frac{2 p_1 \cdot (2\xi - k_1)}{p_1 \cdot p_2 (k_1^2 - 2\xi \cdot k_1)}. \quad (23)$$

Note that the original propagator k_2^2 in the diagram and additional x terms from the limit $k = -x p_1$ are replaced by the last factor in eq. (23), where ξ is an auxiliary vector satisfying $p_1 \cdot \xi$, $\xi^2 \neq 0$. This guarantees that the counterterm captures the correct behavior in the collinear limit $k \parallel p_1$, while ensuring the finiteness in the other collinear limit $k \parallel p_2$. This counterterm integrates to zero due to the Ward identity in eq. (21) and locally removes the collinear singularity $k \parallel p_1$ of the modified shift integrable diagrams. A similar counterterm can be constructed for the other collinear limit $\Delta_2 \mathcal{M}_{gg \rightarrow H, \text{IR}}^{(2), \text{shift}}$. These two counterterms, which take care of the local collinear singularities, can be recast diagrammatically as shift counterterms if a certain choice of the quark loop momentum label l is made. This is explained in more detail in ref. [15].

5. Conclusion and next steps

In these proceedings we presented a framework for the local subtraction of infrared singularities in the two-loop amplitude for gluon-fusion Higgs production. With a “scalar” decomposition of the triple-gluon vertex, one classifies the infrared singular diagrams into two groups, the factorizable diagrams and the shift-integrable diagrams. In addition, the decomposition allows the introduction of a specific loop momentum routing for the gluons. This ensures the local factorization of the factorizable diagrams in the infrared limits via cancellations by Ward identities. The local singularities of the shift-integrable diagrams are removed with local counterterms which leave the integrated value of the amplitude invariant. With these constructions, one can remove all infrared singularities locally with one form factor counterterm times the one-loop amplitude and several shift counterterms, as shown in eq. (4). The sum of all counterterms, which vanish after integration, is

$$\Delta\mathcal{M}_{gg\rightarrow H}^{(2)}(k, l) = \Delta\mathcal{M}_{gg\rightarrow H, \text{IR}}^{(2), \text{fact}}(k, l) + \Delta_s\mathcal{M}_{gg\rightarrow H, \text{IR}}^{(2), \text{shift}} + \Delta_1\mathcal{M}_{gg\rightarrow H, \text{IR}}^{(2), \text{shift}} + \Delta_2\mathcal{M}_{gg\rightarrow H, \text{IR}}^{(2), \text{shift}}. \quad (24)$$

This procedure can be generalized to an arbitrary number of external electroweak bosons in gluon fusion, as described in more detail in ref. [15]. Note that after this procedure, ultraviolet singularities of the the amplitude need to be regularized by additional local counterterms, which can be achieved by Taylor expanding the diagram in the specific limits and truncating at the necessary order with a mass regulator (see more details in ref. [15]). The fully finite amplitude is then suitable for numerical integration. The counterterms eventually must be integrated analytically and added back to the amplitude.

This has been a first exploration of constructing a locally finite two-loop amplitude with incoming gluons. In view of a generalization, one needs to study NNLO processes with initial state gluons that introduce double infrared singularities. Additional issues arise for these amplitudes due to vertex and self-energy corrections next to the external legs. The self-energy corrections introduce power-like collinear singularities, which need to be reduced to logarithmic singularities such that we can rely on a leading-power approximation to write down a factorized counterterm. Vertex corrections next to an initial state produce the so-called *loop polarizations*. Namely, the loop momentum of the correction does not necessarily point in the same direction as the external momentum, which could damage the local factorization in the collinear limits. Local subtractions resolving both problems have to be introduced without changing the integrated value of the full amplitude. These issues were previously solved for electron positron and quark anti-quark annihilation in refs. [13, 14]. For initial state gluons, new loop polarization structures appear, requiring the development of novel methods to systematically tackle these issues. These extensions to the framework of local factorization in momentum space are part of ongoing research.

Acknowledgments

I would like to thank my collaborators on the project in ref. [15], Charalampos Anastasiou, George Sterman and Aniruddha Venkata. I am grateful to Yao Ma for his advice on these proceedings. This work was supported by the Swiss National Science Foundation through its project funding scheme (grant number 10001706).

References

- [1] Heinrich, G. Collider Physics at the Precision Frontier. *Phys. Rept.* **922** pp. 1-69 (2021)
- [2] Huss, A., Huston, J., Jones, S. & Pellen, M. Les Houches 2021—physics at TeV colliders: report on the standard model precision wishlist. *J. Phys. G.* **50**, 043001 (2023)
- [3] Kermanschah, D. & Vicini, M. Numerical integration of the double- and triple-box integrals using threshold subtraction. *Loops And Legs In Quantum Field Theory.* (2024,7)
- [4] Sen, A. Asymptotic Behavior of the Wide Angle On-Shell Quark Scattering Amplitudes in Nonabelian Gauge Theories. *Phys. Rev. D.* **28** pp. 860 (1983)
- [5] Collins, J., Soper, D. & Sterman, G. Factorization of Hard Processes in QCD. *Adv. Ser. Direct. High Energy Phys.* **5** pp. 1-91 (1989)
- [6] Catani, S. The Singular behavior of QCD amplitudes at two loop order. *Phys. Lett. B.* **427** pp. 161-171 (1998)
- [7] Sterman, G. & Tejeda-Yeomans, M. Multiloop amplitudes and resummation. *Phys. Lett. B.* **552** pp. 48-56 (2003)
- [8] Dixon, L., Magnea, L. & Sterman, G. Universal structure of subleading infrared poles in gauge theory amplitudes. *JHEP.* **8** pp. 022 (2008)
- [9] Collins, J. Foundations of perturbative QCD. (Cambridge University Press,2013,11)
- [10] Feige, I. & Schwartz, M. Hard-Soft-Collinear Factorization to All Orders. *Phys. Rev.* **D90**, 105020 (2014)
- [11] Erdoğan, O. & Sterman, G. Ultraviolet divergences and factorization for coordinate-space amplitudes. *Phys. Rev. D.* **91**, 065033 (2015)
- [12] Ma, Y. A Forest Formula to Subtract Infrared Singularities in Amplitudes for Wide-angle Scattering. *JHEP.* **5** pp. 012 (2020)
- [13] Anastasiou, C., Haindl, R., Sterman, G., Yang, Z. & Zeng, M. Locally finite two-loop amplitudes for off-shell multi-photon production in electron-positron annihilation. *JHEP.* **4** pp. 222 (2021)
- [14] Anastasiou, C. & Sterman, G. Locally finite two-loop QCD amplitudes from IR universality for electroweak production. (2022,12)
- [15] Anastasiou, C., Karlen, J., Sterman, G. & Venkata, A. Locally finite two-loop amplitudes for electroweak production through gluon fusion. (2024,3)